HHS Public Access

Author manuscript

Anesthesiology. Author manuscript; available in PMC 2017 September 01.

Published in final edited form as:

Anesthesiology. 2016 September ; 125(3): 535–546. doi:10.1097/ALN.0000000000001213.

α_2-Adrenergic receptor and isoflurane modulation of presynaptic Ca^{2+} influx and exocytosis in hippocampal neurons

Masato Hara, M.D., Ph.D.[1,3], **Zhen-Yu Zhou, M.D., Ph.D.**[1], and **Hugh C. Hemmings Jr., M.D., Ph.D.**[1,2]

[1]Department of Anesthesiology, Weill Cornell Medical College, New York, NY 10065, USA

[2]Department of Pharmacology, Weill Cornell Medical College, New York, NY 10065, USA

[3]Department of Anesthesiology, Kurume University School of Medicine, Kurume, Fukuoka 830-0011, Japan

Abstract

Background—Evidence indicates that the anesthetic-sparing effects of α_2-adrenergic receptor (AR) agonists involve α_{2A}-AR heteroreceptors on non-adrenergic neurons. Since volatile anesthetics inhibit neurotransmitter release by reducing synaptic vesicle (SV) exocytosis, we hypothesized that α_2-AR agonists inhibit non-adrenergic SV exocytosis and thereby potentiate presynaptic inhibition of exocytosis by isoflurane.

Methods—Quantitative imaging of fluorescent biosensors of action potential (AP) evoked SV exocytosis (synaptophysin-pHlourin) and Ca^{2+} influx (GCaMP6) were used to characterize presynaptic actions of the clinically used α_2-AR agonists dexmedetomidine and clonidine, and their interaction with isoflurane, in cultured rat hippocampal neurons.

Results—Dexmedetomidine (0.1 μM, n = 10) or clonidine (0.5 μM, n = 8) inhibited AP-evoked exocytosis (54 ± 5% and 59 ± 8% of control, respectively; $p < 0.001$). Effects on exocytosis were blocked by the subtype-nonselective α_2-AR antagonist atipamezole or the α_{2A}-AR selective antagonist BRL 44408, but not by the α_{2C}-AR selective antagonist JP 1302. Dexmedetomidine inhibited exocytosis and presynaptic Ca^{2+} influx without affecting Ca^{2+} coupling to exocytosis, consistent with an effect upstream of Ca^{2+}-exocytosis coupling. Exocytosis coupled to both N-type and P/Q-type Ca^{2+} channels was inhibited by dexmedetomidine or clonidine. Dexmedetomidine potentiated inhibition of exocytosis by 0.7 mM isoflurane (to 42 ± 5%, compared to 63 ± 8% for isoflurane alone; $p < 0.05$).

Conclusions—Hippocampal SV exocytosis is inhibited by α_{2A}-AR activation in proportion to reduced Ca^{2+} entry. These effects are additive with those of isoflurane, consistent with a role for

Corresponding author: Hugh C. Hemmings, Jr. M.D., Ph.D., Weill Cornell Medical College, Department of Anesthesiology, Box 124, 1300 York Avenue, New York, NY 10065, USA. Phone: (212) 746-2949. hchemmi@med.cornell.edu.

Conflict of Interest: HCH is an Editor of *Anesthesiology* and of the *British Journal of Anesthesia;* All other authors have no conflicts of interest.

Disclosure of funding: This work was supported by NIH grant GM58055 (HCH), and the Departments of Anesthesiology of Weill Cornell Medical College, New York, NY, USA and Kurume University School of Medicine, Kurume, Fukuoka, Japan.

α_{2A}-AR presynaptic heteroreceptor inhibition of non-adrenergic synaptic transmission in the anesthetic-sparing effects of α_{2A}-AR agonists.

Introduction

General anesthesia is a reversible drug-induced state of neurological unresponsiveness characterized by amnesia, unconsciousness and immobility in response to painful stimuli. The molecular and cellular mechanisms that produce these key pharmacological features are poorly understood.[1] All general anesthetics modulate synaptic transmission and neuronal excitability, altering the balance between excitation and inhibition and reducing connectivity in central nervous system networks.[2,3] The principal molecular targets underlying these cellular and network effects include both ligand-gated and voltage-gated ion channels.[1,4] Dexmedetomidine (DEX) and clonidine (CLO) are not general anesthetics themselves, but produce sedative-hypnotic and anesthetic-sparing effects through activation of G protein-coupled α_{2A}-adrenergic receptors (α_{2A}-ARs).[5,6] The downstream targets coupled to α_{2A}-AR activation that contribute to their anesthetic-sparing effects are incompletely characterized.

A well-described effect of α_2-AR agonists is suppression of norepinephrine release from noradrenergic locus coeruleus (LC) neurons through inhibitory autoreceptor activation.[7] This mechanism was originally suggested to underlie the sedative action of DEX.[8] However, genetic analysis of the functional roles of α_2-AR subtypes in adrenergic and non-adrenergic cells indicates that the sedative-hypnotic effects of α_2-AR agonists are mediated not by presynaptic α_{2A}-AR autoreceptors but rather by α_{2A}-AR heteroreceptors on non-adrenergic neurons.[9] Moreover, the cellular locations and actions of these critical non-adrenergic neuronal α_{2A}-ARs responsible for the sedative and anesthetic-sparing actions of α_2-AR agonists are unknown.[10]

Volatile anesthetics are known to inhibit the release of multiple neurotransmitters through direct presynaptic mechanisms, including more potent inhibition of the release of glutamate, the principal excitatory neurotransmitter in the central nervous system, compared to other neurotransmitters.[11–14] Since α_2-AR agonists reduce requirements for general anesthetics,[15] we hypothesized that they also affect non-adrenergic synaptic transmission through presynaptic effects on evoked neurotransmitter release. Reduced excitatory transmission resulting in alteration of the balance between neuronal excitation and inhibition has been implicated in the effects volatile anesthetics,[1,16] and provides a plausible mechanism for the well known pharmacological interaction underlying the anesthetic-sparing effects of α_2-AR agonists.

α_{2A}-ARs are expressed widely in neurons throughout the central nervous system,[17,18] primarily at presynaptic rather than postsynaptic sites,[9,19] consistent with a role for presynaptic α_{2A}-ARs on non-adrenergic neurons in their neuropharmacological effects. Suppression of both excitatory and inhibitory neurotransmission by α_2-AR agonists has been shown by electrophysiological recordings in brain slices,[20,21] but since neurotransmitter release was not measured directly, these synaptic effects could be mediated postsynaptically or indirectly through intrinsic noradrenergic afferents rather than by direct

presynaptic actions on heterosynaptic α_{2A}-ARs. We therefore studied the effects and α_2-AR receptor subtype specificity of the clinically used α_2-AR agonists DEX and CLO and their pharmacodynamic interaction with isoflurane on action potential (AP)-evoked synaptic vesicle (SV) exocytosis and presynaptic Ca^{2+} influx in cultured rat hippocampal neurons using quantitative biosensor fluorescence live-cell imaging approaches[22–24].

Materials and Methods

Reagents and solutions

Dexmedetomidine (DEX), clonidine (CLO), atipamezole, BRL 44408, and JP 1302 were purchased from Tocris Bioscience (Bristol, UK); ω-conotoxin GIVA and ω-agatoxin IVA from Alomone Labs (Jerusalem, Israel); bafilomycin A1 from Calbiochem (San Diego, CA), and isoflurane from Abbott (Chicago, IL). All other reagents were purchased from Sigma-Aldrich (St. Louis MO). The synaptophysin-pHluorin (syn-pH) construct was kindly provided by Yongling Zhu (Northwestern University, Chicago, IL), and the GCaMP6 construct was kindly provided by Loren L. Looger (Janelia Farm Research Campus, Howard Hughes Medical Institute, Ashburn VA).[24]

Isoflurane-saturated stock solutions (~12 mM) were prepared and diluted daily into gas-tight glass syringes, from which a sample was taken for determination of aqueous isoflurane concentration. Solutions were perfused focally onto imaged cells *via* a 150-μm diameter perfusion pipette using polytetrafluoroethylene tubing to minimize isoflurane loss. Concentrations used corresponded to 1–3 times the minimum alveolar concentration (MAC) in rat corrected to 30°C (0.35 mM).[25] Perfusate samples were taken at the tip of the perfusion manifold to determine delivered isoflurane concentrations, and reflected ~10% loss from the syringe to the pipette tip. Isoflurane concentrations were determined by extraction into *n*-heptane (1:1 v/v) followed by analysis using a Shimadzu GC-2010 Plus gas chromatograph (Tokyo, Japan) with external standard calibration.[26]

Hippocampal neuron culture and transfection

Experiments were approved by the Weill Cornell Medical College Institutional Animal Care and Use Committee and conformed to NIH Guidelines for the Care and Use of Animals. Hippocampal CA3–CA1 regions were dissected from neonatal Sprague-Dawley rats (1–3 days old, ♂ and ♀), and cells were dissociated and plated as described.[22] Neurons were transfected on DIV 7–8 with the syn-pH or GCaMP6 construct using the Ca_2PO_4 method, and imaging experiments were conducted on DIV 14–21.[23] Randomization was not used to assign experimental conditions as the pharmacologcal approaches used required specific sequential applications of drugs, therefore the experimenter was not blinded to the conditions. Rat pups born from at least three different parents were used for each set of experiments.

Synaptic vesicle exocytosis

Synaptophysin-pHlourin (syn-pH), a fusion protein of the engineered pH-sensitive green fluorescent protein pHluorin fused to the lumenal N-terminal tail of the synaptic vesicular protein synaptophysin, was used as an optical biosensor of SV exocytosis.[22,27] Changes in

fluorescence (ΔF) during electrical stimulation of AP firing reflect alkalization of pHlourin due to exocytosis, while changes during the post-stimulus period reflect re-acidification following endocytosis.[22] The transfection method yielded only several transfected cells per dish due to the low transfection efficiency such that boutons from single cells could be identified and imaged without interference from other neurons.

Live-cell imaging was performed at 30.0 ± 0.2°C with continuous superperfusion at 0.27 ml min^{-1} with Tyrode's solution containing (in mM) 119 NaCl, 2.5 KCl, 2 $CaCl_2$, 2 $MgCl_2$, 25 HEPES buffered to pH 7.4, and 30 glucose, with 10 μM 6-cyano-7-nitroquinoxaline-2,3-dione (CNQX) and 50 μM D,L-2-amino-5-phosphonovaleric acid (AP5) included to block excitatory synaptic transmission and recurrent excitation. Fluorescence images were acquired with an Andor iXon1 camera (model DU-897E-BV; South Windsor, CT) with a solid-state diode pumped 488 nm laser shuttered using acousto-optic modulation. Data were acquired at 10 or 100 Hz by integrating for 30 or 9.74 ms in frame transfer mode and restricting imaging to a sub-area of the CCD chip. The ΔF for exocytosis in response to AP trains was defined as the difference between the average of 2–10 frames before and after the stimulus.

Action potentials (APs) were evoked by stimulation with 1-ms current pulses yielding fields of ~10 V cm^{-1} using platinum-iridium electrodes. Cells were allowed to rest for ~60 s between 1–20 AP trains and at least 5 min between 10 Hz 200–600 AP trains. Experiments were followed by a maximally depleting stimulus (1200 APs at 10 Hz) in the presence of the v-ATPase inhibitor bafilomycin A1 (0.5 μM), which prevents SV re-acidification following exocytosis, to determine total recycling pool (TRP) size, and then by perfusion with 50 mM NH_4Cl (substituted for 50 mM NaCl and buffered to pH 7.4) to define the total pool (TP) by alkalization of all vesicles. Fluorescence measurements are expressed as a fraction of the TP (Figure 1).[23]

Calcium measurements

GCaMP6 was used to measure intracellular Ca^{2+} ($[Ca^{2+}]_i$) in hippocampal neuron boutons stimulated by field-potential-generated APs in the presence of 2 mM extracellular Ca^{2+} ($[Ca^{2+}]_e$).[24] GCaMP6 peak fluorescence (ΔF) for each stimulus was determined by averaging the two highest points post-stimulation and subtracting the average baseline of 10 points prior to AP stimulation.

Image and Statistical Analysis

Boutons were selected for analysis by demonstrating their responsiveness to test applications of NH_4Cl. Peak amplitude at 100 APs was selected at 10 s in the middle of a 10 Hz 20 s stimulation. Bafilomycin A1 and NH_4Cl effects were analyzed as mean plateau values. Images were analyzed in ImageJ (http://rsb.info.nih.gov/ij) with a custom plug-in (http://rsb.info.nih.gov/ij/plugins/time-series.html). Silent boutons, defined as those where the response to 100 APs was smaller than the standard deviation of the baseline before stimulation ($\Delta F_{100} - \sigma \leq 0$), were excluded from analysis; < 10% of boutons did not respond to stimulation and were excluded from analysis. Based on previous studies,[13,14,22,23] sample sizes of ≥ 5 were used. Data are shown as mean ± s.e.m. ANOVA with Tukey or Bonferroni

post hoc tests, two-tailed Student's *t*-test ($p < 0.05$), and 95% confidence intervals were used for testing statistical significance. GraphPad Prism 6 (GraphPad Software, Inc., San Diego, CA) was used for statistical analysis.

Results

α_2-AR agonists inhibit synaptic vesicle exocytosis

The effects of α_2-AR agonists on SV exocytosis were studied using live-cell imaging of cultured rat hippocampal neurons. Exocytosis evoked by 60 s of field electrical stimulation at a frequency of 10 Hz across 25–40 boutons led to a rapid increase in fluorescence due to exocytosis and externalization of syn-pH (Fig. 1B). Blocking re-acidification with bafilomycin A1 led to a plateau in fluorescence at ~200 s identifying the total recycling pool (TRP) size (Fig. 1C). Signals were normalized at each bouton to the total pool (TP) obtained by rapid alkalization of the entire labeled vesicle pool using NH_4Cl (Fig. 1C), thus correcting signals for variations in syn-pH expression levels. The time course of the fluorescence change during a train of 600 APs averaged over a population of individual boutons from a single transfected neuron is shown in Fig. 1D. Fluorescence reached a peak that decayed after the stimulus period due to endocytosis and SV re-acidification (Fig. 1D).

AP-evoked exocytosis was inhibited by the clinically used sedative α_2-AR agonists DEX (0.1 μM; Fig. 1B, D, E) or CLO (0.5 μM; Fig. 1F, G), concentrations known to be effective *in vitro*.[21,28] The more selective α_2-AR agonist DEX applied for 15 min reduced peak exocytosis elicited by 100 APs to 54 ± 5% of control (95% CI [0.42, 0.65], Fig. 1E), with no significant difference in effect between 2 min and 15 min of DEX application indicating a rapid onset of inhibition. The less selective partial α_2-AR agonist CLO inhibited peak SV exocytosis to 59 ± 8% of control (95% CI [0.40, 0.78], Fig. 1G). The degree of inhibition of SV exocytosis was less at the end of 60 s of stimulation (600 AP) compared to 10 s of stimulation (100 AP) for DEX (95% CI [−0.21, −0.01], $p = 0.04$ by two-tailed paired *t*-test, n = 10) or CLO (95% CI [−0.36, −0.05], $p = 0.016$ by two-tailed paired *t*-test, n = 8), indicating that inhibition can be partially overcome by a longer stimulation period (Fig. 1E, G). During prolonged stimulation in the presence of bafilomycin A1, neither DEX (0.59 ± 0.03, 95% CI [0.51, 0.67], $p = 0.95$, n = 10) nor CLO (0.61 ± 0.03, 95% CI [0.54, 0.68], $p = 0.76$, n = 8) affected TRP size as a fraction of TP compared to control (0.60 ± 0.03, 95% CI [0.53, 0.66], n = 11, by two-tailed unpaired *t*-test; data not shown).

Inhibition of exocytosis is mediated by the α_{2A}-AR subtype

There are three major α_2-AR receptor subtypes: α_{2A}, α_{2B}, and α_{2C}.[29] The specific subtype mediating inhibition of SV exocytosis by DEX and CLO was examined using subtype-selective antagonists. DEX (0.1 μM) reduced peak exocytosis elicited by 100 AP to 57 ± 6% of control (95% CI [0.43, 0.71], n = 9, Fig. 2A). The nonselective α_2-AR antagonist atipamezole (APZ) abolished inhibition of SV exocytosis by DEX, indicating a specific α_2-AR receptor-mediated mechanism (n = 7, Fig. 2B). Treatment with the α_{2A}-AR selective antagonist BRL 44408 (1 μM) also blocked inhibition by DEX (n = 8, Fig. 2C), while the α_{2C}-AR selective antagonist JP 1302 (3 μM) had no effect on inhibition of exocytosis by DEX (n = 7, Fig. 2D). Similar receptor subtype selectivity was observed for CLO (data not

shown). These findings indicate that DEX and CLO inhibit SV exocytosis exclusively through interaction with of α_{2A}-ARs.

The effects of DEX and CLO on exocytosis evoked by increasing numbers of APs were also investigated (Fig. 3A). Peak exocytosis increased incrementally from 1 to 20 AP stimuli. The degree of inhibition by DEX was comparable across this range of stimuli (57 – 60% of control, n = 7, Fig. 3B), with inhibition to 60 ± 6% of control at 20 APs (95% CI [0.35, 0.80]). Similar results were observed for 0.5 μM CLO (58 – 65% of control, n = 9, data not shown).

α_2-AR agonists inhibit exocytosis by reducing Ca^{2+} influx

Increases in intracellular Ca^{2+} ($[Ca^{2+}]_i$) were measured in hippocampal boutons using the optogenetic fluorescent reporter GCaMP6 as an indicator of presynaptic Ca^{2+} influx.[24] Peak $[Ca^{2+}]_i$ increased incrementally from 1 to 20 AP stimuli (Fig. 3C). The degree of inhibition by DEX was comparable across this range of stimuli (55 – 62% of control, n = 6, Fig. 3D), with 62 ± 3% of control at 20 APs (95% CI [0.48, 0.78]), comparable to the degree of inhibition of SV exocytosis. Similar results were observed for 0.5 μM CLO (63 – 74% of control, n = 8, data not shown).

Correlation between AP-evoked SV exocytosis and Ca^{2+} influx was measured over a range of AP stimuli to quantify the efficiency of exocytosis at different degrees of Ca^{2+} influx (Ca^{2+}-exocytosis coupling). The relationship between paired exocytosis-Ca^{2+} influx data for DEX overlapped control data (Fig. 4), confirming that the effect of DEX on SV exocytosis is directly proportional to reduction in Ca^{2+} influx with no measurable effect on the Ca^{2+}-sensitivity of exocytosis.

While N-type voltage gated Ca^{2+} channels (VGCCs) are closely coupled to depolarization-evoked release of norepinephrine in sympathetic neurons,[30,31] SV exocytosis in non-adrenergic neurons involves contributions from both N- and P/Q-type VGCCs.[32–35] We used VGCC subtype-specific peptide neurotoxins to evaluate the roles of N- and P/Q-type VGCCs in the inhibitory effects of DEX on hippocampal SV exocytosis (Fig. 5). The specific N-type VGCC blocker ω–conotoxin GIVA inhibited exocytosis to 62 ± 9% of control (95% CI [0.40, 0.83]) following 10 s of 10 Hz stimulation at 2 mM extracellular Ca^{2+} ($[Ca^{2+}]_e$). Treatment with DEX further inhibited exocytosis to 47 ± 10% of control (95% CI [0.22, 0.72]), consistent with an effect of DEX on exocytosis mediated by P/Q-type channels (n = 7, Fig. 5A). The specific P/Q-type VGCC toxin ω-agatoxin IVA inhibited SV exocytosis to 53 ± 10% of control (95% CI [0.29, 0.78]). Treatment with DEX further inhibited exocytosis to 33 ± 7% of control (95% CI [0.17, 0.49]), consistent with an effect of DEX on exocytosis mediated by uninhibited N-type channels as well (n = 8, Fig. 5B). Thus DEX inhibits exocytosis mediated by the two major presynaptic VGCC subtypes known to be coupled to SV exocytosis in the hippocampus.[32–35] Similar results were observed for 0.5 μM CLO (data not shown).

Presynaptic interaction between dexmedetomidine and isoflurane

Clinical features of α_2-AR agonists include their ability to produce sedation and to increase the potency of general anesthetics (anesthetic-sparing effect).[5,6] Since volatile anesthetics

such as isoflurane also inhibit SV exocytosis in hippocampal neurons,[1,13,14] we studied the interaction between isoflurane (ISO) and DEX in suppressing exocytosis (Fig. 6). ISO inhibited exocytosis in a concentration-dependent manner (n = 5, Fig. 6A): 2 MAC ISO inhibited exocytosis to 63 ± 8 % of control (95% CI [0.45, 0.82]); addition of 0.1 μM DEX further inhibited exocytosis to 42 ± 5% of control (95% CI [0.31, 0.53], n = 7, Fig. 6B), greater than the effect of DEX alone (54 ± 5%, 95% CI [0.42, 0.65]; Fig. 1E). The effect of ISO did not involve activation of α_2-ARs as it was not prevented by the subtype nonselective α_2-AR antagonist atipamezole, which also had no effect on exocytosis alone (n = 7, Fig. 6C).

Discussion

Noradrenergic signaling plays important roles in controlling the endogenous sleep-awake cycle and general anesthesia,[36] but the mechanisms involved in the interaction between general anesthetics and the anesthetic-sparing effects of α_2-AR agonists are unclear. Potentiation of general anesthesia (anesthetic sparing) is a characteristic neuropharmacological effect of α_{2A}-AR agonists.[5,6,37] A well known action of α_{2A}-AR agonists is their modulation of norepinephrine release through presynaptic autoreceptors (receptors for the same transmitter released by the neuron), but elegant genetic studies targeting cell specific α_2-AR receptor expression indicate that classical presynaptic noradrenergic neuron autoreceptor effects are not involved in this anesthetic-sparing action.[9,10] Here we show that the α_2-AR agonists DEX and CLO inhibit SV exocytosis and Ca^{2+} entry in non-adrenergic hippocampal neurons by a heteroreceptor (receptors for a transmitter not released by the neuron) α_{2A}-AR–mediated effect. Moreover, this mechanism is additive with inhibition of SV exocytosis by the volatile anesthetic isoflurane (for summary of possible mechanisms see Fig. 7).

Advances in fast microscopic imaging and sensitive fluorescent biosensors allowed us to determine the effects of α_2-AR agonists on both AP-evoked SV exocytosis[22,23,27] and Ca^{2+} influx[24] in intact central nervous system neurons without interference from noradrenergic innervation. We observed that the clinically used α_2-AR agonists DEX and CLO inhibited SV exocytosis from hippocampal neurons through activation of α_{2A}-ARs to reduce Ca^{2+} influx mediated by both N-type and P/Q-type VGCCs. Moreover, the highly selective α_2-AR agonist DEX potentiated the presynaptic effects of isoflurane to reduce SV exocytosis. This provides a putative presynaptic target for the anesthetic-sparing properties of α_2-AR agonists,[6] a clinically relevant pharmacological interaction that allows reduced dosing of general anesthetics to mitigate their dangerous side-effect profiles.[37]

Contrary to our findings, conventional electrophysiological studies have not detected DEX or medetomidine effects on basal neurotransmission of Schaffer collaterals in rat hippocampus.[38,39] Field excitatory postsynaptic potentials (fEPSPs) are the sum of individual signals from many cells, including inhibitory GABArgic interneurons that have extensive arbors that innervate pyramidal cells. Individual GABArgic interneurons can powerfully inhibit thousands of excitatory pyramidal neurons. Activity of postsynaptic neurons also contributes to fEPSPs such that fEPSPs are affected both by inhibitory signals from GABArgic interneurons and by postsynaptic mechanisms, possibly explaining the

insensitivity of the fEPSP to the effects of DEX. In contrast, the method we used selectively reports activity from presynaptic boutons of only a single cell, most commonly nonGABAergic neurons as detected by vGAT immunoreactivity.[14] Although we did not routinely determine neuronal phonotype at the time of this study, we did screen 29 of the 96 neurons described here using vGAT-Oyster labeling, and all 29 were negative (i.e. not GABAergic and thus assumed to be glutamatergic; data not shown). Further studies of neurons of defined transmitter phenotype will be necessary to determine whether there are transmitter-specific differences in α_{2A}-AR modulation of SV exocytosis.

We have shown previously that isoflurane inhibits SV exocytosis in hippocampal neurons.[13,14] While the effects of DEX and isoflurane on exocytosis are additive, their molecular mechanisms are distinct since the isoflurane effect is insensitive to α_2-AR antagonism. The inhibitory effects of volatile anesthetics on hippocampal exocytosis are thus independent of α_2-AR coupled G protein signaling, but rather appear to involve primarily direct depression of presynaptic voltage-gated Na^+ channels (Na_v) to reduce presynaptic excitability.[13,40] In contrast, the sedative and anesthetic-sparing properties of α_2-AR agonists are mediated by G protein-coupled receptors, specifically through the $G\alpha_{i2}$ isoform.[41] The relevant G protein-regulated downstream targets for the presynaptic effects of α_2-AR agonists on Ca^{2+} influx and in turn SV exocytosis remain to be established. CLO can inhibit both N- and P/Q-type Ca^{2+} currents in mouse amygdala slices, consistent with our findings of effects on both pathways of Ca^{2+} entry.[42] Moreover, a recent study shows that DEX inhibits $Na_v1.8$ currents in rat dorsal root ganglion neurons by increasing activation threshold and decreasing AP firing, suggesting that α_{2A}-AR agonists might also affect AP frequency and propagation.[43] These parallel pathways of inhibition result in additive effects of isoflurane and α_2-AR agonists on both Ca^{2+} influx and SV exocytosis, thus providing a plausible cellular mechanism for their pharmacodynamic anesthetic-sparing interactions *in vivo*.[9,10] Electrophysiological studies or optical measurements of action potential waveforms using microbial rhodopsin-based biosensors[44] should allow further studies to determine directly whether α_{2A}-AR agonists affect presynaptic AP properties.

The α_2-ARs were among the first presynaptic receptors identified by their role as autoreceptors coupled to inhibition of norepinephrine release.[29] Previous studies suggested that the sedative and anesthetic-sparing effects of selective α_2-AR agonists involved reductions in noradrenergic neurotransmission through autoreceptor activation.[45] However, more recent studies have implicated effects of α_2-AR agonists on non-adrenergic neurons in these actions.[9,46,47] Genetically engineered mice that express α_{2A}-ARs only in noradrenergic terminals show minimal neurological effects of the α_2-AR agonist medetomidine, including loss of righting reflex and anesthetic-sparing, in contrast to a strong hypnotic effect in wild-type littermates.[9] In another study *in vivo,* acute knockdown of α_{2A}-AR expression in the locus coeruleus failed to affect DEX induced sedation.[46] These findings suggest that α_{2A}-ARs on non-adrenergic neurons mediate their sedative effects. Furthermore, dopamine-β-hydroxylase knockout mice that have no synaptic norepinephrine release show enhanced sensitivity to and delayed emergence from DEX-induced hypnosis compared to wild-type mice.[47] This further supports the concept that norepinephrine release from locus coeruleus neurons is not critical for DEX-induced hypnosis, but rather supports a role for direct α_2-AR agonist actions on non-adrenergic neurons in their sedative and

anesthetic-sparing actions. Our findings demonstrate a presynaptic site of interaction between the volatile anesthetic isoflurane and the highly selective α_2-AR agonist DEX in reducing SV exocytosis by blocking Ca^{2+} influx in hippocampal neuron axon terminals, a mechanism previously implicated in the presynaptic anesthetic actions of volatile anesthetics.[13,14]

The role of presynaptic α_2-AR agonist-mediated inhibition of neurotransmitter release from non-adrenergic neurons in specific anesthetic endpoints is compelling, but identification of the relevant neuronal networks involved will require further study. The hypnotic effects of α_2-AR agonists were initially proposed to be mediated by presynaptic α_{2A}-ARs on noradrenergic projections from the locus coeruleus to mimic endogenous sleep mechanisms.[45,48] While indirect neurophysiological studies *in vivo* continue to invoke this mechanism,[49] genetic studies provide strong evidence that non-adrenergic, not noradrenergic, α_{2A}-ARs mediate the sedative, hypnotic and anesthetic-sparing actions of α_2-AR agonists.[9,10,46,47] Plausible targets for the hypnotic and anesthetic-sparing effects of α_2-AR agonists include direct suppression of synaptic transmission in cortico-cortical[3] and thalamo-cortical networks.[48,49] A recent study *in vivo* using the TetTag-hM_3D_q system to record and reactivate neuronal groups activated by DEX implicates the preoptic hypothalamus and neighboring dorsal structures in DEX-induced sedation.[46]

Although our studies were conducted in hippocampal neurons, and are therefore most directly relevant to the amnestic properties of the α_2-AR agonist DEX,[50,51] the effects observed involve fundamental mechanisms regulating SV exocytosis in all neurons.[52] Given the widespread expression of α_{2A}-AR receptors,[17,18] this pharmacodynamic interaction is likely to apply throughout the central nervous system. Identification of the locations of the specific non-adrenergic α_{2A}-ARs involved in the multiple neuropharmacological endpoints essential for enhancing general anesthetic effects is critical to development of more targeted agents with improved specificity and therefore safety. Modulation of synaptic transmission by α_{2A}-ARs might also contribute to their emerging organoprotective effects, further augmenting their clinical utility by both reducing anesthetic doses and preserving organ function.[53]

Acknowledgments

We thank Drs. Loren L. Looger Ph.D. of Janelia Research Campus, Howard Hughes Medical Institute, Ashburn, VA, USA and Yongling Zhu Ph.D., Assistant Professor of Ophthalmology, Northwestern University, Chicago, IL, USA for generously providing plasmids. We also thank members of the Hemmings and Ryan laboratories (WCMC, New York, NY, USA) for constructive interactions and critical reading of the manuscript.

References

1. Hemmings HC, Akabas MH, Goldstein PA, Trudell JR, Orser BA, Harrison NL. Emerging molecular mechanisms of general anesthetic action. Trends Pharmacol Sci. 2005; 26:503–10. [PubMed: 16126282]
2. Hudetz AG. General anesthesia and human brain connectivity. Brain Connect. 2012; 2:291–302. [PubMed: 23153273]
3. Alkire MT, Hudetz AG, Tononi G. Consciousness and anesthesia. Science. 2008; 322:876–80. [PubMed: 18988836]

4. Franks NP. General anaesthesia: from molecular targets to neuronal pathways of sleep and arousal. Nat Rev Neurosci. 2008; 9:370–86. [PubMed: 18425091]
5. Segal IS, Vickery RG, Walton JK, Doze VA, Maze M. Dexmedetomidine diminishes halothane anesthetic requirements in rats through a postsynaptic alpha 2 adrenergic receptor. Anesthesiology. 1988; 69:818–23. [PubMed: 2848424]
6. Lakhlani PP, MacMillan LB, Guo TZ, McCool BA, Lovinger DM, Maze M, Limbird LE. Substitution of a mutant α_{2a}-adrenergic receptor via "hit and run" gene targeting reveals the role of this subtype in sedative, analgesic, and anesthetic-sparing responses in vivo. Proc Natl Acad Sci USA. 1997; 94:9950–5. [PubMed: 9275232]
7. Gilsbach R, Hein L. Presynaptic metabotropic receptors for acetylcholine and adrenaline/noradrenaline. Handb Exp Pharmacol. 2008; 184:261–88. [PubMed: 18064417]
8. Correa-Sales C, Rabin BC, Maze M. A hypnotic response to dexmedetomidine, an α_2 agonist, is mediated in the locus coeruleus in rats. Anesthesiology. 1992; 76:948–52. [PubMed: 1350889]
9. Gilsbach R, Ro C, Beetz N, Brede M, Hadamek K, Haubold M, Leemhuis J, Philipp M, Schneider J, Urbanski M, Szabo B, Weinshenker D, Hein L. Genetic dissection of α2-adrenoceptor functions in adrenergic versus nonadrenergic cells. Mol Pharmacol. 2009; 75:1160–70. [PubMed: 19251826]
10. Gilsbach R, Hein L. Are the pharmacology and physiology of α_2 adrenoceptors determined by α_2-heteroreceptors and autoreceptors respectively? Br J Pharmacol. 2012; 165:90–102. [PubMed: 21658028]
11. Westphalen RI, Hemmings HC. Volatile anesthetic effects on glutamate versus GABA release from isolated rat cortical nerve terminals: 4-aminopyridine-evoked release. J Pharmacol Exp Ther. 2006; 316:216–23. [PubMed: 16174800]
12. Westphalen RI, Desai KM, Hemmings HC. Presynaptic inhibition of the release of multiple major central nervous system neurotransmitter types by the inhaled anaesthetic isoflurane. Br J Anaesth. 2013; 110:592–9. [PubMed: 23213036]
13. Hemmings HC, Yan W, Westphalen RI, Ryan TA. The general anesthetic isoflurane depresses synaptic vesicle exocytosis. Mol Pharmacol. 2005; 67:1591–9. [PubMed: 15728262]
14. Baumgart JP, Zhou ZY, Hara M, Cook DC, Hoppa MB, Ryan TA, Hemmings HC. Isoflurane inhibits synaptic vesicle exocytosis through reduced Ca^{2+} influx, not Ca^{2+} -exocytosis coupling. Proc Natl Acad Sci USA. 2015; 112:11959–64. [PubMed: 26351670]
15. Scholz J, Tonner PH. α2-Adrenoceptor agonists in anaesthesia: a new paradigm. Curr Opin Anaesthesiol. 2000; 13:437–42. [PubMed: 17016338]
16. MacIver MB. Anesthetic agent-specific effects on synaptic inhibition. Anesth Analg. 2014; 119:558–69. [PubMed: 24977633]
17. Nicholas A, Pieribone V, Hökfelt T. Distributions of mRNAs for alpha-2 adrenergic receptor subtypes in rat brain: an in situ hybridization study. J Comp Neurol. 1993; 328:575–94. [PubMed: 8381444]
18. Winzer-Serhan UH, Raymon HK, Broide RS, Chen Y, Leslie FM. Expression of alpha 2 adrenoceptors during rat brain development-I. α_{2A} messenger RNA expression. Neuroscience. 1997; 76:241–60. [PubMed: 8971775]
19. Milner TA, Lee A, Aicher SA, Rosin DL. Hippocampal α_{2A}-adrenergic receptors are located predominantly presynaptically but are also found postsynaptically and in selective astrocytes. J Comp Neurol. 1998; 395:310–27. [PubMed: 9596526]
20. Shields AD, Wang Q, Winder DG. α_{2A}-adrenergic receptors heterosynaptically regulate glutamatergic transmission in the bed nucleus of the stria terminalis. Neuroscience. 2009; 163:339–51. [PubMed: 19527774]
21. Nakamura M, Suk K, Lee MG, Jang IS. α_{2A} adrenoceptor-mediated presynaptic inhibition of GABAergic transmission in rat tuberomammillary nucleus neurons. J Neurochem. 2013; 125:832–42. [PubMed: 23570239]
22. Sankaranarayanan S, Ryan TA. Real-time measurements of vesicle-SNARE recycling in synapses of the central nervous system. Nat Cell Biol. 2000; 2:197–204. [PubMed: 10783237]
23. Kim SH, Ryan TA. CDK5 serves as a major control point in neurotransmitter release. Neuron. 2010; 67:797–809. [PubMed: 20826311]

24. Chen TW, Wardill TJ, Sun Y, Pulver SR, Renninger SL, Baohan A, Schreiter ER, Kerr Ra, Orger MB, Jayaraman V, Looger LL, Svoboda K, Kim DS. Ultrasensitive fluorescent proteins for imaging neuronal activity. Nature. 2013; 499:295–300. [PubMed: 23868258]
25. Taheri S, Halsey MJ, Liu J, Eger EI, Koblin DD, Laster MJ. What solvent best represents the site of action of inhaled anesthetics in humans, rats, and dogs? Anesth. Analg. 1991; 72:627–34.
26. Ratnakumari L, Hemmings HC. Inhibition of presynaptic sodium channels by halothane. Anesthesiology. 1998; 88:1043–54. [PubMed: 9579514]
27. Kavalali ET, Jorgensen EM. Visualizing presynaptic function. Nat Neurosci. 2014; 17:10–6. [PubMed: 24369372]
28. Brum PC, Hurt CM, Shcherbakova OG, Kobilka B, Angelotti T. Differential targeting and function of α_{2A} and α_{2C} adrenergic receptor subtypes in cultured sympathetic neurons. Neuropharmacology. 2006; 51:397–413. [PubMed: 16750543]
29. Starke K. Presynaptic autoreceptors in the third decade: focus on α_2-adrenoceptors. J Neurochem. 2001; 78:685–93. [PubMed: 11520889]
30. Hirning LD, Fox AP, McCleskey EW, Olivera BM, Thayer SA, Miller RJ, Tsien RW. Dominant role of N-type Ca2+ channels in evoked release of norepinephrine from sympathetic neurons. Science. 1988; 239:57–61. [PubMed: 2447647]
31. Boehm S, Huck S. Inhibition of N-type calcium channels: the only mechanism by which presynaptic alpha 2-autoreceptors control sympathetic transmitter release. Eur J Neurosci. 1996; 8:1924–31. [PubMed: 8921283]
32. Wheeler DB, Randall A, Tsien RW. Roles of N-type and Q-type Ca2+ channels in supporting hippocampal synaptic transmission. Science. 1994; 264:107–11. [PubMed: 7832825]
33. Reuter H. Measurements of exocytosis from single presynaptic nerve terminals reveal heterogeneous inhibition by Ca^{2+}-channel blockers. Neuron. 1995; 14:773–9. [PubMed: 7718239]
34. Wu LG, Saggau P. Pharmacological identification of two types of presynaptic voltage-dependent calcium channels at CA3-CA1 synapses of the hippocampus. J Neurosci. 1994; 14:5613–22. [PubMed: 8083757]
35. Ariel P, Hoppa MB, Ryan TA. Intrinsic variability in Pv, RRP size, Ca^{2+} channel repertoire, and presynaptic potentiation in individual synaptic boutons. Front Synaptic Neurosci. 2013; 4:9. [PubMed: 23335896]
36. Sanders RD, Maze M. Noradrenergic trespass in anesthetic and sedative states. Anesthesiology. 2012; 117:945–7. [PubMed: 23042229]
37. Aantaa R, Jaakola ML, Kallio A, Kanto J. Reduction of the minimum alveolar concentration of isoflurane by dexmedetomidine. Anesthesiology. 1997; 86: 1055–60. [PubMed: 9158354]
38. Takamatsu I, Iwase A, Ozaki M, Kazama T, Wada K, Sekiguchi M. Dexmedetomidine reduces long-term potentiation in mouse hippocampus. Anesthesiology. 2008; 108:94–102. [PubMed: 18156887]
39. Ribeiro PO, Antunes LM, Nunes CS, Silva HB, Cunha RA, Tomé ÂR. The effects of different concentrations of the α_2-adrenoceptor agonist medetomidine on basal excitatory synaptic transmission and synaptic plasticity in hippocampal slices of adult mice. Anesth Analg. 2015; 120:1130–7. [PubMed: 25658314]
40. Herold KF, Hemmings HC. Sodium channels as targets for volatile anesthetics. Front Pharmacol. 2012; 3:1–7. [PubMed: 22291651]
41. Gilsbach R, Piekorz RP, Pexa K, Beetz N, Schneider J, Nu B, Birnbaumer L, Hein L. Modulation of α_2-adrenoceptor functions by heterotrimeric $G_{\alpha i}$ protein isoforms. J Pharmacol Exp Ther. 2009; 331:35–44. [PubMed: 19589951]
42. DeBock F, Kurz J, Azad SC, Parsons CG, Hapfelmeier G, Zieglgansberger W, Rammes G. α_2-Adrenoreceptor activation inhibits LTP and LTD in the basolateral amygdala: involvement of $G_{i/o}$-protein-mediated modulation of Ca^{2+}-channels and inwardly rectifying K^+-channels in LTD. Eur J Neurosci. 2003; 17:1411–24. [PubMed: 12713644]
43. Gu XY, Liu BL, Zang KK, Yang L, Xu H, Pan HL, Zhao ZQ, Zhang YQ. Dexmedetomidine inhibits Tetrodotoxin-resistant Nav1.8 sodium channel activity through Gi/o-dependent pathway in rat dorsal root ganglion neurons. Mol Brain. 2015; 8:15 1–11. [PubMed: 25761941]

44. Hoppa MB, Gouzer G, Armbruster M, Ryan TA. Control and plasticity of the presynaptic action potential waveform at small CNS nerve terminals. Neuron. 2014; 84: 778–789. [PubMed: 25447742]
45. Nelson LE, Lu J, Guo T, Saper CB, Franks NP, Maze M. The α_2-adrenoceptor agonist dexmedetomidine converges on an endogenous sleep-promoting pathway to exert its sedative effects. Anesthesiology. 2003; 98:428–36. [PubMed: 12552203]
46. Zhang Z, Ferretti V, Güntan, Moro A, Steinberg EA, Ye Z, Zecharia AY, Yu X, Vyssotski AL, Brickley SG, Yustos R, Pillidge ZE, Harding EC, Wisden W, Franks NP. Neuronal ensembles sufficient for recovery sleep and the sedative actions of α2 adrenergic agonists. Nat Neurosci. 2015; 18:553–61. [PubMed: 25706476]
47. Hu FY, Hanna GM, Han W, Mardini F, Thomas SA, Wyner AJ, Kelz MB. Hypnotic hypersensitivity to volatile anesthetics and dexmedetomidine in dopamine β-hydroxylase knockout mice. Anesthesiology. 2012; 117:1006–17. [PubMed: 23042227]
48. Huupponen E, Maksimow A, Lapinlampi P, Särkelä M, Saastamoinen A, Snapir A, Scheinin H, Scheinin M, Meriläinen P, Himanen S-L, Jääskeläinen S. Electroencephalogram spindle activity during dexmedetomidine sedation and physiological sleep. Acta Anaesthesiol Scand. 2008; 52:289–294. [PubMed: 18005372]
49. Akeju O, Loggia ML, Catana C, Pavone KJ, Vazquez R, Rhee J, Contreras Ramirez V, Chonde DB, Izquierdo-Garcia D, Arabasz G, Hsu S, Habeeb K, Hooker JM, Napadow V, Brown EN, Purdon PL. Disruption of thalamic functional connectivity is a neural correlate of dexmedetomidine-induced unconsciousness. Elife. 2014; 3:1–23.
50. Pryor KO, Reinsel RA, Mehta M, Li Y, Wixted JT, Veselis RA. Visual P2-N2 complex and arousal at the time of encoding predict the time domain characteristics of amnesia for multiple intravenous anesthetic drugs in humans. Anesthesiology. 2010; 113:313–26. [PubMed: 20613477]
51. Hayama HR, Drumheller KM, Mastromonaco M, Reist C, Cahill LF, Alkire MT. Event-related functional magnetic resonance imaging of a low dose of dexmedetomidine that impairs long-term memory. Anesthesiology. 2012; 117:981–95. [PubMed: 22929730]
52. Dittman J, Ryan TA. Molecular circuitry of endocytosis at nerve terminals. Annu Rev Cell Dev Biol. 2009; 25:133–60. [PubMed: 19575674]
53. Sanders RD, Xu J, Shu Y, Januszewski A, Halder S, Fidalgo A, Sun P, Hossain M, Ma D, Maze M. Dexmedetomidine attenuates isoflurane-induced neurocognitive impairment in neonatal rats. Anesthesiology. 2009; 110:1077–85. [PubMed: 19352168]

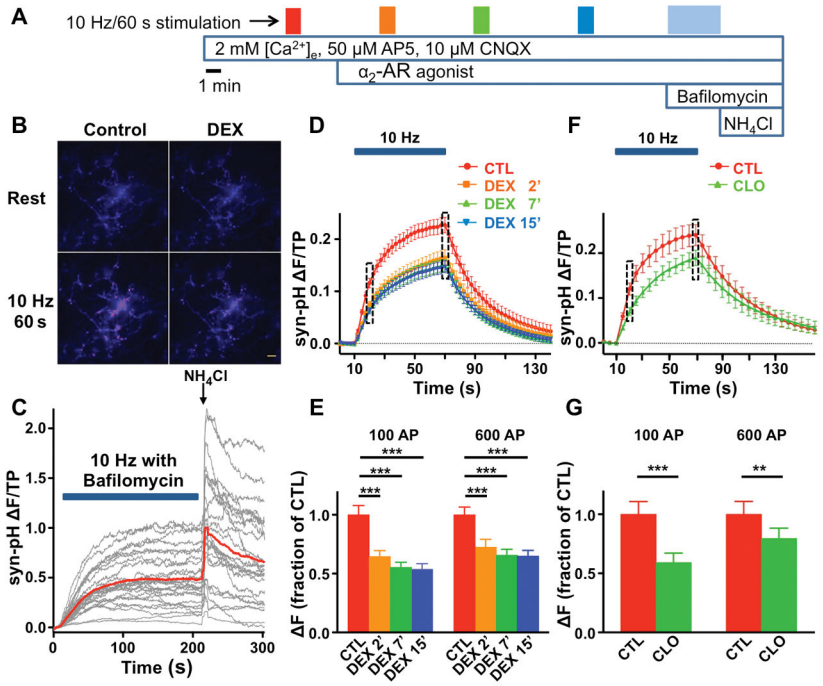

Figure 1. α_2-Adrenergic receptor agonists inhibit action potential-evoked synaptic vesicle exocytosis from hippocampal neurons

A, Schematic diagram of protocol to test the effects of α_2-adrenergic receptor (AR) agonists on synaptic vesicle (SV) exocytosis. Filled boxes indicate electrical stimulation at 10 Hz for 60 s (600 action potentials (APs)), followed by 3 cycles of 600 AP stimuli in the presence of the α_2-AR agonists 0.1 μM dexmedetomidine (DEX) or 0.5 μM clonidine (CLO) with at least 5 min rest between each stimulation. **B**, Representative fluorescence images of synaptophysin-pHluorin (syn-pH) expressing boutons at rest (upper panels) and after 600 APs (lower panels) for control (left) and DEX-treated neurons (right). Scale bar, 10 μm. **C**, Representative traces (gray) and average (red) of syn-pH fluorescence to determine total recycling pool (TRP) size and total pool (TP) obtained from 26 boutons analyzed from a single neuron were stimulated continuously at 10 Hz (bar indicates electrical stimulation) in the presence of 0.5 μM bafilomycin A1 to prevent SV re-acidification. The plateau in fluorescence reflects TRP. Vesicle alkalization with 50 mM NH_4Cl revealed the size of the TP. **D**, Time series of fluorescence changes, shown every 2.5 s, for 600 APs in the absence (Control) or presence of 0.1 μM DEX (following 2, 7, and 15 min drug exposure). Fluorescence intensities were normalized to the subsequent NH_4Cl response (TP). Bar indicates electrical stimulation. **E**, Mean values of peak syn-pH response amplitude at 10 s (100 APs) and 60 s (600 APs) of stimulation (boxed areas in D), normalized to control values for each time point. Data are expressed as mean ± SEM. $^{***}p < 0.001$ by one-way repeated measures ANOVA followed by Tukey's multiple comparison test. **F,** Time series of fluorescence changes, shown every 5 s, for 600 APs in the absence or presence of 0.5 μM CLO (following 7 min exposure). **G**, Mean values of peak syn-pH response amplitude at 10 s (100 AP) and 60 s (600 AP) of stimulation (boxed areas in F), normalized to control values for each time point. Data are expressed as mean ± SEM. $^{**}p < 0.01$, $^{***}p < 0.001$ compared to respective control by two-tailed paired *t*-test.

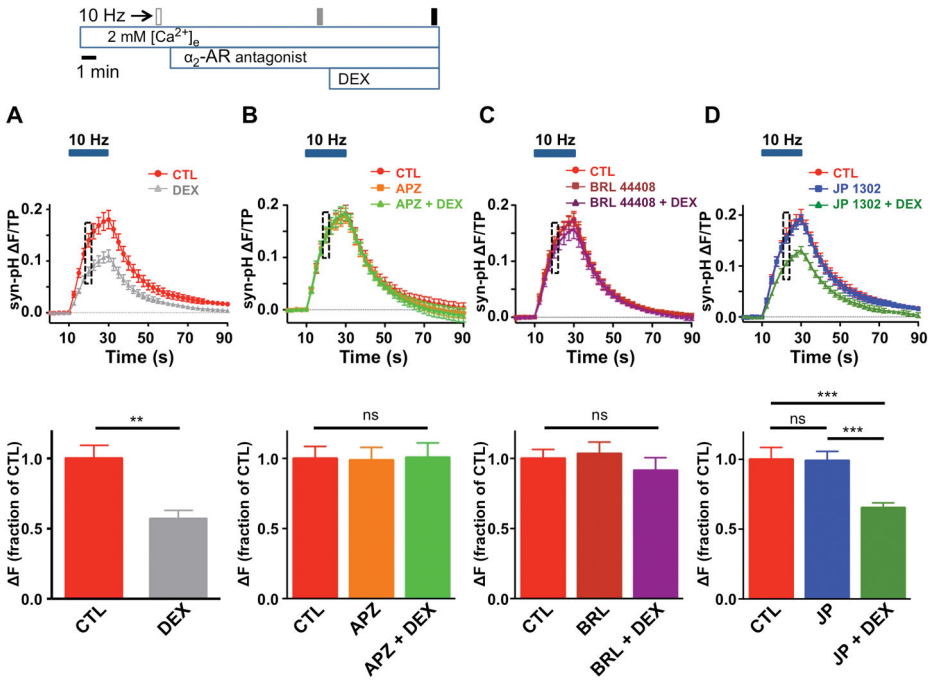

Figure 2. Effects of α_2-adrenergic receptor antagonists on dexmedetomidine inhibition of synaptic vesicle exocytosis

Top, Schematic diagram of protocol to test the effect of dexmedetomidine (DEX) on synaptophysin-pHluorin (syn-pH) fluorescence in the presence of α_2-adrenergic receptor (AR) antagonists. Filled boxes indicate electrical stimulation at 10 Hz for 20 sec. **A**, *Top*, Time series of fluorescence changes in the absence (Control) or presence of DEX applied for 7 min, shown every 2.5 s, normalized to total pool (TP) before and after stimulation (horizontal bar). *Bottom*, Mean effect of 0.1 μM DEX on synaptic vesicle (SV) exocytosis at 10 sec of stimulation (DEX 57 ± 6% of control). Data are expressed as mean ± SEM. $^{**}p < 0.01$ by two-tailed paired *t*-test (n = 9). **B–D**, Effects of α_2-AR antagonists on action potential (AP)-evoked SV exocytosis at 10 s of stimulation (boxes). *Top*, Fluorescence changes with time before and after stimulation. Fluorescence intensities normalized to TP, with data shown every 2.5 s. *Bottom*, ΔF at 10 s of stimulation. Data are expressed as mean ± SEM. $^{***}p < 0.001$; ns, not significant by one-way repeated measures ANOVA followed by Tukey's multiple comparison test.

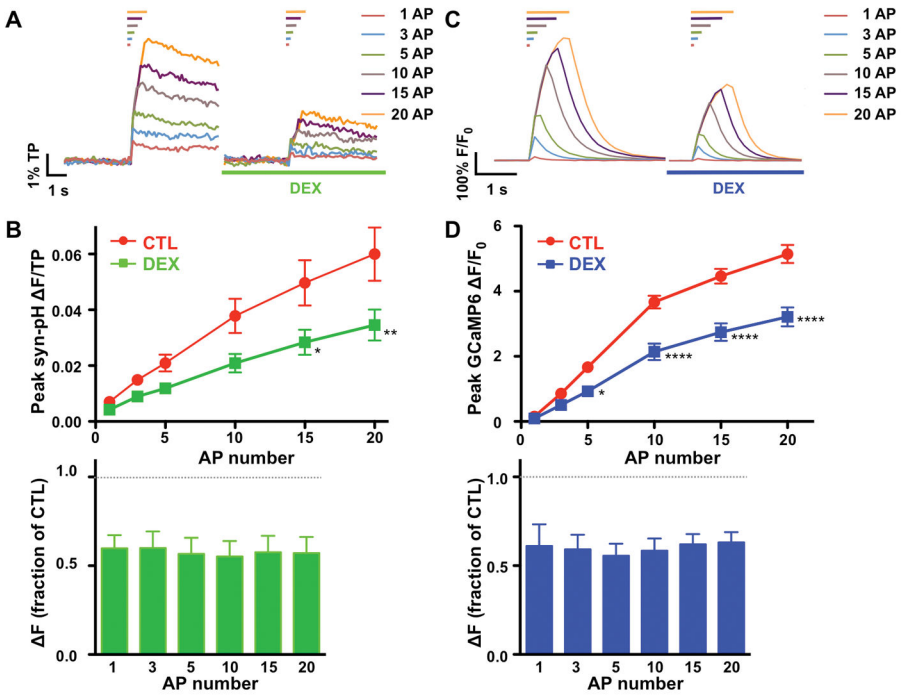

Figure 3. Effect of dexmedetomidine on synaptic vesicle exocytosis and presynaptic Ca^{2+} influx in response to increasing stimuli

A, Representative synaptophysin-pHluorin (syn-pH) fluorescence responses of a single cell relative to total pool (TP) size evoked by 1, 3, 5, 10, 15 and 20 APs in 2 mM $[Ca^{2+}]_e$ for control (*left traces*) or in the presence of 0.1 μM dexmedetomidine (DEX) applied for 7 min after control recording (*right traces*). Bars on top indicate duration of 20 Hz stimuli. Each trace was averaged from 1–5 trials of 25–40 boutons. Scale bar = 1% TP, 1 s. **B**, Inhibition of synaptic vesicle (SV) exocytosis by DEX. *Top*, Peak syn-pH response as a function of action potential (AP) number in the absence (Control) or presence of DEX (0.1 μM) Data are expressed as mean ± SEM. *$p < 0.05$, **$p < 0.01$ compared to control by two-way repeated measures ANOVA with Bonferroni *post hoc* test (n = 7). *Bottom*, Mean peak responses of syn-pH normalized to each control response (no significant differences by one-way ANOVA). **C**, Representative GCaMP6 fluorescence responses elicited by 1, 3, 5, 10, 15 and 20 APs in 2 mM $[Ca^{2+}]_e$ for control (*left traces*) or in the presence of 0.1 μM DEX (*right traces*) applied for 7 min after control recording. Bars on top indicate duration of 20 Hz AP stimuli. Each trace was averaged from 1–5 trials of 25~40 boutons. Scale bar = 100% $\Delta F/F_0$, 1 s. **D**, Inhibition of presynaptic Ca^{2+} influx by DEX. *Top*, Peaks of GCaMP6 response as a function of AP number (1, 3, 5, 10, 15 and 20 APs) in the absence (Control) or presence of DEX (0.1 μM). Data are expressed as mean ± SEM. *$p < 0.01$, ****$p < 0.0001$ compared to control by two-way repeated measures ANOVA with Bonferroni *post hoc* test (n = 6). *Bottom*, Mean peak responses of GCaMP6 normalized to control for each AP number (no significant difference by one-way ANOVA).

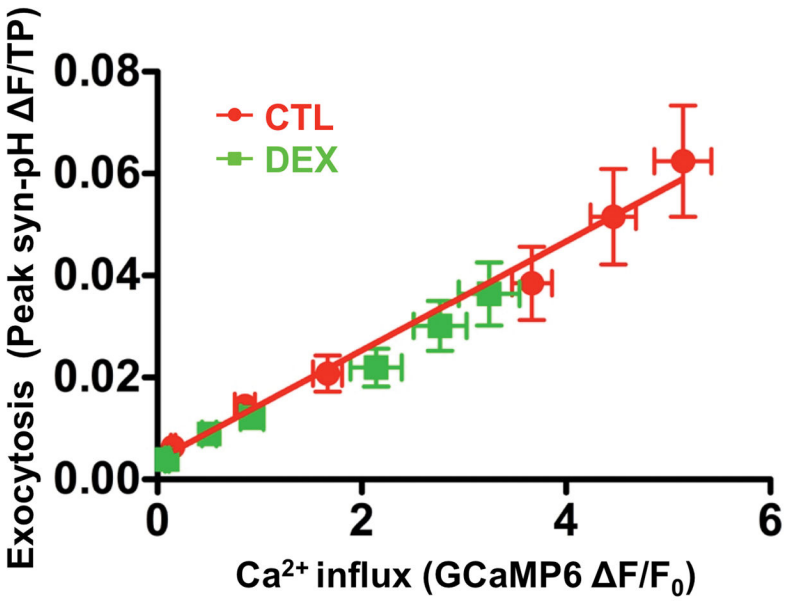

Figure 4. Dexmedetomidine reduces Ca^{2+} influx and synaptic vesicle exocytosis without affecting the Ca^{2+} sensitivity of exocytosis

Exocytosis plotted as a function of Ca^{2+} influx in the absence (control) or presence of 0.1 μM dexmedetomidine (DEX) combining data for synaptic vesicle (SV) exocytosis (from Fig. 3B) with data for Ca^{2+} influx (from Fig. 3D) for 1–20 AP stimuli. Data are fitted to a linear model (exocytosis = 0.0107 ± 0.0014$[Ca^{2+}]_i$ – 0.00389±0.00458).

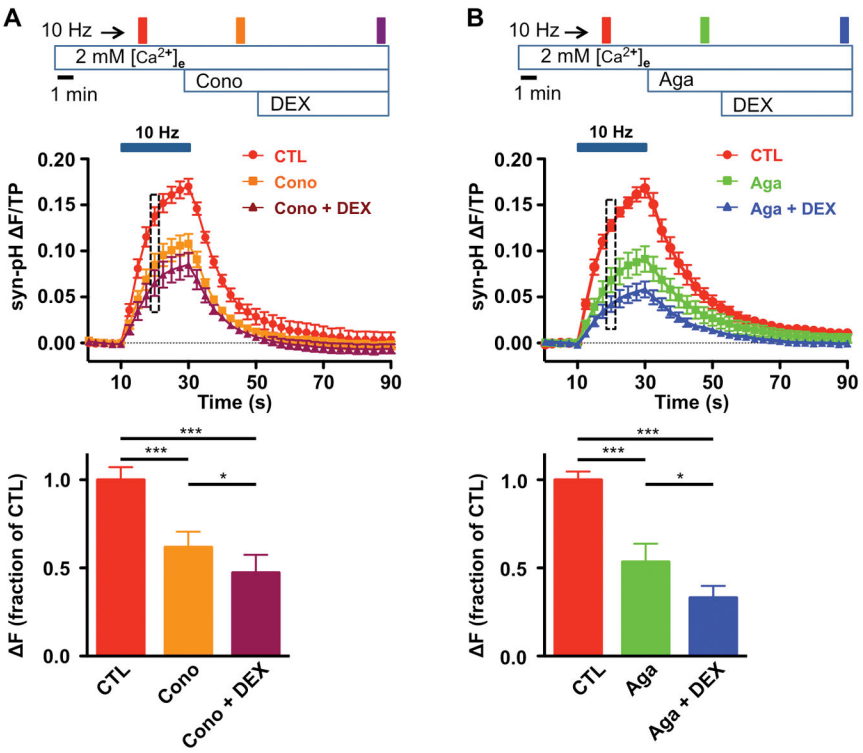

Figure 5. Voltage-gated Ca^{2+} channel subtypes contributing to modulation of exocytosis by dexmedetomidine

A, Effect of 0.1 μM dexmedetomidine (DEX) on exocytosis in the presence of the selective N-type voltage-gated Ca^{2+} channel (VGCC) antagonist ω-conotoxin GIVA (Cono, 1 μM). *Top*, Schematic diagram of protocol. *Middle*, Time series of fluorescence changes with stimulation at 10 Hz for 20 sec. Fluorescence was normalized to TP with data shown every 2.5 s. *Bottom*, Mean amplitudes of synaptophysin-pHluorin (syn-pHy) responses at 10 s of 10 Hz stimulation normalized to control (n = 7). **B,** Effect of 0.1 μM DEX in the presence of the specific P/Q-type VGCC antagonist ω-agatoxin IVA (Aga, 0.4 μM). *Top*, Schematic diagram of protocol. *Middle*, Time series of fluorescence change with 20 s stimulation at 10 Hz. Fluorescence was normalized to TP with data shown every 2.5 s. *Bottom*, Mean amplitudes of syn-pH responses at 10 s AP of 10 Hz stimulation normalized to control (n = 8). Data are expressed as mean ± SEM. *$p < 0.05$, ***$p < 0.001$ by one-way repeated measures ANOVA followed by Tukey's multiple comparison test.

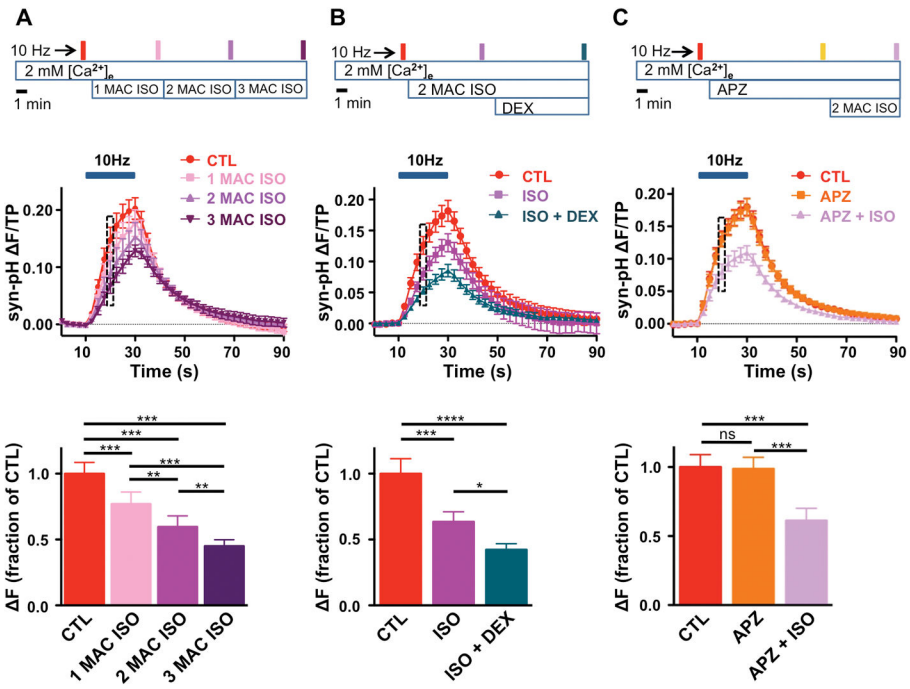

Figure 6. Dexmedetomidine potentiates isoflurane inhibition of action potential-evoked synaptic vesicle exocytosis

A, *Top*, Schematic diagram of protocol. Filled boxes indicate 20 s of 10 Hz electrical stimulation with sequential exposure to 1 minimum alveolar concentration (MAC, 0.35 mM), 2 MAC or 3 MAC isoflurane (ISO) for 5 min. *Middle*, Time series of synaptophysin-pHluorin (syn-pH) fluorescence changes, shown every 2.5 s, normalized to total pool (TP) before and after 20 s stimulation at 10 Hz. *Bottom*, Mean effect of ISO on synaptic vesicle (SV) exocytosis at 10 s of stimulation (box) normalized to control (n = 5). **B**, Effects of 0.1 μM dexmedetomidine (DEX) in the presence of 2 MAC ISO on *action potential* (AP)-evoked SV exocytosis at 20 s of 10 Hz stimulation. *Top*, Schematic diagram of protocol. *Middle*, Time series of syn-pH fluorescence changes, shown every 2.5 s, normalized to TP before and after 20 s stimulation at 10 Hz. *Bottom*, Mean effect of ISO and ISO + DEX on SV exocytosis at 10 s of stimulation (box) normalized to control (n = 7). **C**, Effects of the nonselective α_2-adrenergic receptor (AR) antagonist atipamezole (APZ; 1 μM) on 2 MAC ISO inhibition of AP-evoked SV exocytosis at 10 s of 10 Hz stimulation. *Top*, Schematic diagram of protocol. *Middle*, Time series of fluorescence changes, shown every 2.5 s, normalized to TP before and after 20 s stimulation at 10 Hz. *Bottom*, Mean effect of APZ and APZ + ISO on SV exocytosis at 10 s of stimulation (box) normalized to control (n = 7). Data are expressed as mean ± SEM. *$p < 0.05$, **$p < 0.01$, ***$p < 0.001$, ****$p < 0.0001$, ns, not significant by one-way repeated measures ANOVA followed by Tukey's multiple comparison test.

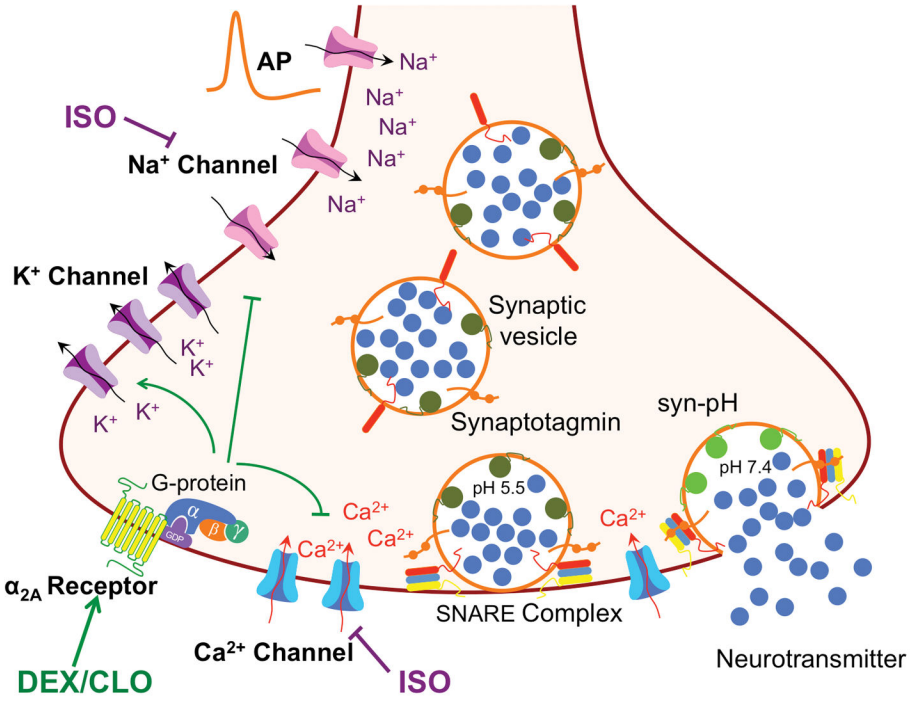

Figure 7.

Presynaptic mechanisms relevant to the effects of α_2-adrenergic receptor agonists on synaptic vesicle exocytosis. Inhibition by the volatile anesthetic isoflurane (ISO) is due primarily to inhibition of voltage-gated Na^+ channels (Na_v) rather than direct inhibition of voltage-gated Ca^{2+} channels (Ca_v) or SNARE proteins. Effects of α_{2A}-adrenergic receptor (AR) agonists such as dexmedetomidine (DEX) and clonidine (CLO) are mediated by G-protein-coupled receptors, specifically through the $G\alpha_{i2}$ isoform. The relevant downstream targets of G-protein activation by α_{2A}-AR are unknown; plausible candidates include activation of K^+ channels, inhibition of Ca_v, and/or by reduced action potential (AP)-induced depolarization through inhibition of Na_v. Use of the fluorescent biosensor synaptophysin-pHlourin (syn-pH; green circles) to measure exocytosis is also shown; increased fluorescence is induced by the increase in pH following synaptic vesicle fusion (right).